Journal of Basic Physical Research ISSN: 2141-8403 Prints, 2141-8411 Online
Vol.14, Issue 2, October, 2025, pp. 214– 222, Available online at https://journals.unizik.edu.ng/jbpr/

SYNTHESIS OF ALUMINIUM DOPED ZINC SELENIDE (ZnSe:Al) THIN FILMS USING CHEMICAL BATH DEPOSITION TECHNIQUE

Isi, P.O[1]*., Emumejaye, K[2]., Ibe C.S[1]., Isah, J[3]. Uzor, C. E.[1]., Ikenga, O.A[1]., Muomeliri, C.B[1]., Aribodor D.N[4]

[1]Department of Physics and Industrial Physics, Nnamdi Azikiwe University, Awka, Anambra State. Nigeria.
[2]Department of Physics, Delta State University of Science and Technology, Ozoro. Nigeria
[3]Department of Physics, University of Abuja. Nigeria
[4]Department of Parasitology and Entomology, Nnamdi Azikiwe University, Awka, Anambra State. Nigeria.
Affiliation: TETFund Centre of Excellence in Biomedicine, Engineering and Agricultural Translation Studies, Nnamdi Azikiwe University.
Correspondence e-mail address: po.isi@unizik.edu.ng

Abstract
Aluminium-doped zinc selenide (ZnSe:Al) thin films were synthesized using the chemical bath deposition technique. Their optical characteristics were examined with a Cary 300 UV–Visible spectrophotometer over the 200–800 nm wavelength range at normal incidence. Absorbance data obtained from the spectrophotometer were used to compute and plot the corresponding transmittance and reflectance spectra. Structural properties were analyzed using a Rigaku Miniflex 630 X-ray diffractometer, while elemental composition was investigated with a JEOL JSM-7600F system. The deposited films exhibited strong absorption in the UV region and relatively weak absorption within the visible range. Surface morphology revealed that increasing aluminum concentration influences grain size, whereas structural analysis indicated that higher Al doping levels progressively suppress the crystalline nature of the films. This indicates that the deposited films are suitability for UV-blocking or optoelectronic applications.
Keywords: *Aluminium-doped Zinc Selenide (ZnSe:Al), Chemical bath, thin films, optical characteristics, X-ray diffraction*

Introduction

The rapid expansion of industrial activities has led to the release of large quantities of toxic gases into the atmosphere, contributing significantly to climate change and various environmental and health challenges [Isi *et al,* 2021, Okoli 2012, Hawar *et al,* 2024]. If these emissions continue unchecked, the resulting climatic shifts are expected to intensify the frequency of extreme weather events such as heat waves, heavy rainfall, storms, and coastal flooding. Addressing these issues requires the development of new and sustainable technologies, particularly in the field of energy production.

Energy supply continues to be a significant challenge for developing countries such as Nigeria, where electricity generated from hydroelectric and geothermal sources is not adequate to satisfy the nation's energy needs. To address this shortfall, there is a strong need to invest in alternative and renewable energy sources. Among the available options, solar energy stands out as one of the most promising. In contrast to non-renewable resources, solar energy is plentiful, environmentally friendly, and sustainable. Nevertheless, its widespread adoption relies on the development and availability of efficient and affordable solar cell technologies.

Solar cells are semiconductor devices capable of converting sunlight directly into electricity [Kassim *et al,* 2011]. The sun delivers solar radiation to the Earth's surface at an estimated rate of approximately 1.4 kW/m² [Gueymard 2004.]. Harnessing this energy through photovoltaic devices enables the generation of renewable electrical power. The history of solar

cell development dates back to 1839 when Becquerel first observed the photovoltaic effect in an electrolytic cell [Jérôme, 2025]. Later, in 1894, Fritts produced the first solar cell using selenium coated with a thin gold layer [Nelson 2003]. Modern solar cells typically consist of a p–n junction formed between a negatively doped (n-type) semiconductor rich in conduction-band electrons and a positively doped (p-type) semiconductor containing holes in its valence band. A key requirement for any solar cell material is its ability to absorb a broad spectrum of photons within the visible region of solar radiation. One of such material that meets these criteria is zinc selenide (ZnSe) [Sagadevan *et al*, 2016, Cansu *et al*, 2025,].

Zinc selenide is a light-yellow, odourless, polycrystalline compound occurring naturally as the mineral stilleite, though it is generally insoluble in water. Chemically represented as ZnSe, it is a II–VI semiconductor with a wide direct band gap of approximately 2.7 eV [Isi *et al*, 2023, Cansu *et al*, 2025, Xia *et al*, 2015, Zhang *et al* 2016, Atikur, 2014, Pankove 1991, Nasir 2025,]. ZnSe exists in two primary crystalline forms—cubic (zinc blende), which is the most stable at ambient conditions, and hexagonal (wurtzite)—making it a notable example of polymorphism. Although rare in nature, ZnSe is commonly synthesized through the reaction of zinc vapour and hydrogen selenide (H_2Se), often forming sheet-like structures on graphite susceptors. ZnSe has found extensive application in optoelectronic devices, including light-emitting diodes (LEDs), ultraviolet (UV) detectors, and laser systems. Its large band gap makes it particularly suitable as a window layer in solar cell structures, where transparency to visible light is crucial [Gemechis *et al*, 2021]. Additionally, ZnSe is widely used in the manufacturing of infrared optical components such as lenses, prisms, and mirrors, and is employed in high-resolution thermal imaging systems due to its favourable optical properties.

This research is on the synthesis of Al-doped ZnSe thin films using different dopant concentrations to study the Surface morphology, optical and structural properties of the grown films.

Materials and Methods

Aluminum-doped zinc selenide thin films were deposited using the following solvents and reagents: zinc acetate dihydrate, aluminum chloride, selenium dioxide, concentrated hydrochloric acid, acetone and distilled water. The apparatus used for this research include beakers, magnetic stirrer hot plate(85-2), Digital M-metlar balance, thermostat water bath HH-6, syringes, spatula, glass substrates, slide clip, slide rack, detergent, storage containers, pair of hand glove, mouth and nose mask, filter paper, and petri dish.

Methodology

Prior to the preparation of the chemical baths, all equipment—including beakers, syringes, and the magnetic stirrer—were thoroughly washed with detergent and rinsed with distilled water. The glass substrates were similarly cleaned using detergent, rinsed with distilled water, soaked in acetone, and then air-dried to ensure the removal of any contaminants.

Stock molar solutions consisting of 0.1 M aluminum chloride**,** 0.3 M selenium dioxide**,** and 0.3 M zinc acetate dihydrate were used in the preparation of the chemical baths. The required volumes of each reagent were measured using separate syringes designated for each compound to avoid cross-contamination. After the addition of each reagent, the solution was stirred to ensure clarity and homogeneity.

For chemical bath 1, 9.8 ml of zinc acetate dihydrate was introduced as the zinc ion source, followed by 2 ml of concentrated HCl, which served as a complexing agent to slow the reaction rate. Subsequently, 19.6 ml of selenium dioxide was added as the selenide ion source, and 0.2 ml of aluminum chloride solution was incorporated to supply aluminum ions while 18.4 ml of

distilled water was used to top it up to 50 ml. This procedure was repeated five times for five different chemical bath to prepare the various chemical baths with differing reagent concentrations.

Clean glass substrates were immersed vertically at the center of each bath, ensuring they did not touch the walls of the container. The chemical baths were then placed in a thermostatic water bath preheated to 90°C, and the deposition process was allowed to proceed for 1 hour for all the reaction chemical bath**.**

Upon completion of the deposition period (1 hour), the substrates were removed, air-dried, and stored in labelled petri dishes for subsequent characterization. Below 1 is the table for variation of various concentrations of reagents at 90ºC.

Table 1. Variation of various concentrations of reagents at 90 ºC.

Reagents	**Volume (ml)**				
	Bath 1	Bath 2	**Bath 3**	**Bath 4**	**Bath 5**
Zinc Acetate dehydrate	9.8	9.6	9.4	9.2	9.0
Conc. HCl	2	4	4	8	10.0
Selenium Dioxide	19.6	19.2	18.8	18.4	18.0
Aluminum Chloride	0.2	0.4	0.6	0.8	1.0
Distilled water	18.4	16.8	15.2	13.6	12.0
Time	1hr	1hr	1hr	1hr	1hr

Observation

During the preparation of the chemical bath, the initially colourless zinc acetate dihydrate solution developed a slight yellow tint upon the addition of concentrated hydrochloric acid. When selenium dioxide was introduced, the solution reverted to a colourless state, which it retained throughout the remainder of the preparation process. During deposition, as the bath containing the immersed substrate was heated, the solution emitted a noticeable pungent odor. Following the completion of deposition, the solution exhibited a colour change from a faint pink hue to a brownish appearance.

Precaustions

i. The glass substrates were thoroughly cleaned with detergent, rinsed with water, soaked in acetone, and finally rinsed with distilled water ensure they were free from contaminations prior to deposition.
ii. All prepared molar solutions were stirred adequately to obtain clear and homogeneous mixtures.
iii. The digital mettler balance was properly zeroed before each weighing to ensure accurate mass measurements.
iv. Double approximation was avoided during mathematical calculations to minimize computational errors.
v. Volumes measured using syringes and beakers were read at the lower meniscus to prevent parallax errors.

Results and Discusion

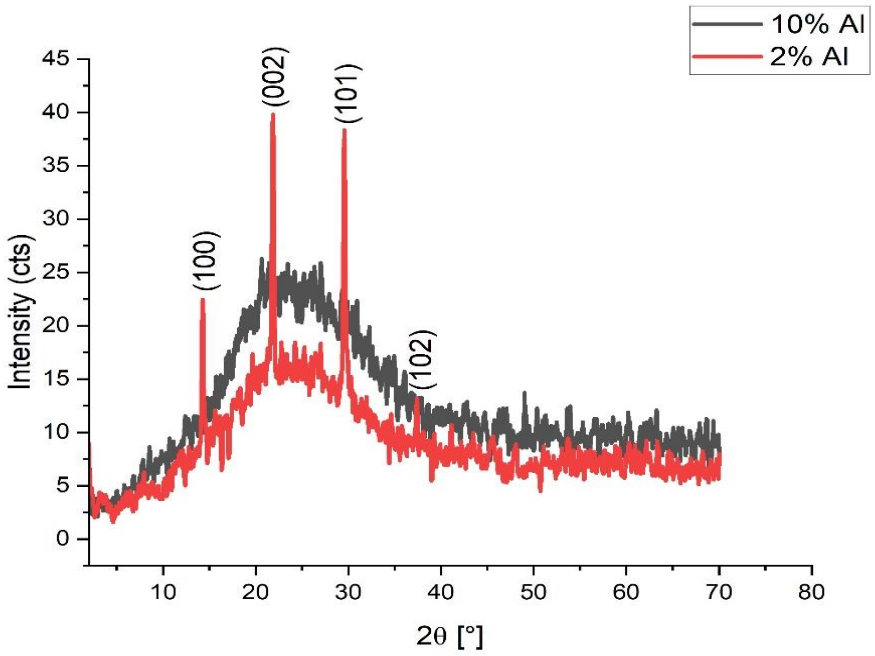

Fig 4.1: XRD graph of the AlZnSe thin films for Samples containing 10% and 2% of Al
XRD Result

The aluminum-doped zinc selenide (ZnSe:Al) thin films were analyzed using X-ray diffraction (XRD) to determine their structural properties. The diffraction patterns were obtained with a Rigaku Miniflex 630 diffractometer. Figure 4.1 presents the XRD profiles of the films containing 2% and 10% aluminum. The diffraction patterns indicate that the deposited ZnSe:Al films exhibit a crystalline structure consisting predominantly of the cubic phase, with a minor contribution from the hexagonal (wurtzite) phase. The presence of hexagonal ZnSe is confirmed by reflections corresponding to the (002) and (101) planes, which are characteristic of the wurtzite structure.

The film doped with 2% Al shows a higher degree of crystallinity and strong texturing, evidenced by four prominent diffraction peaks. These peaks appear at: $2\theta = 14.28°$**,** indexed to the (100) plane, $2\theta = 21.88°$, corresponding to the (002) plane, $2\theta = 29.58°$, associated with the (101) plane, and $2\theta = 37.40°$, attributed to the (102) plane.
In contrast, the film containing 10% Al exhibits only two notable peaks: $2\theta = 21.44°$ for the (002) plane, and $2\theta = 27.00°$ for the (101) plane.

The significant reduction in the number and intensity of peaks with increasing aluminium concentration suggests that higher Al doping levels suppress the crystallinity of the ZnSe thin films, leading to a more disordered or less well-defined structure.

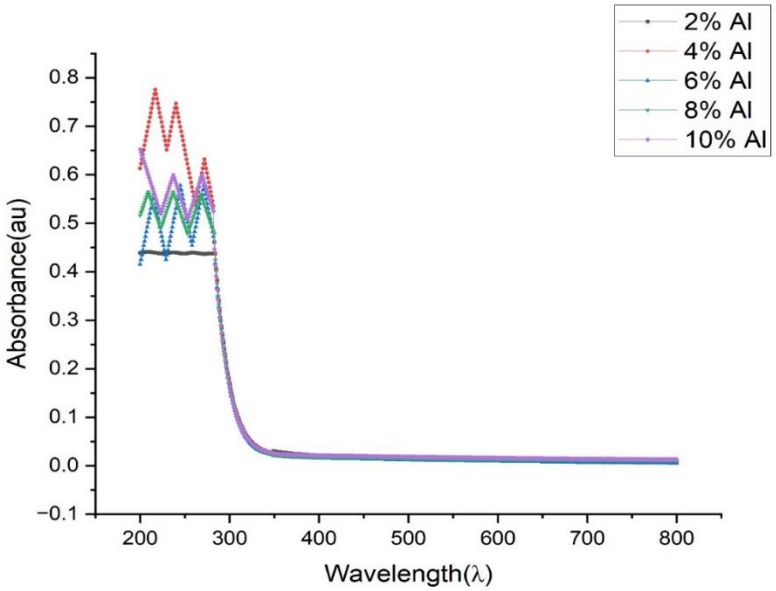

Fig 4.2: A graph of Absorbance (au) against wavelength (λ)

Figure 4.2 displayed high absorbance in the ultraviolet region of the electromagnetic spectrum, while very poor absorbance was displayed in visible region of the electromagnetic spectrum. Though, the sample which contains 4% of Al displayed highest absorption peak. Hence, the sample can be used as a good absorbing materials for solar cells, photo detectors, thermal insulation, medical imaging etc. Therefore, ZnSe:Al thin films are strongly absorbing at wavelengths shorter than 300 nm. This makes the thin films fit for application in solar cells since its fundamental absorption lies within the ultraviolet range. These results agree with those obtained by Rastkar *et al* [Rastkar *et al* 2009]. While Low visible absorbance suggests good transparency in the visible region. Aluminium concentration influences UV absorbance peaks, but has minimal impact on visible-light absorption.

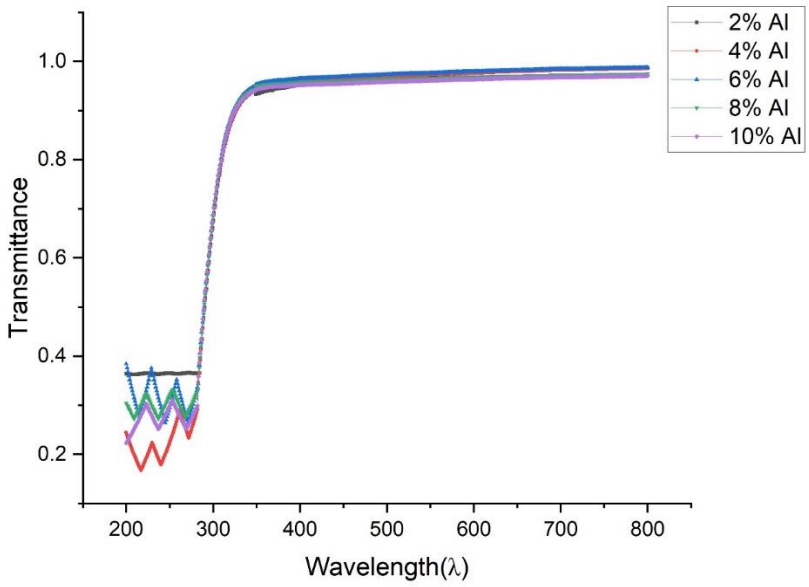

Fig 4.3: A graph of Transmittance against wavelength

The graph shows the transmittance spectra of aluminum-doped zinc selenide (ZnSe:Al) thin films with aluminum concentrations of 2%, 4%, 6%, 8%, and 10%**,** measured over 200–800 nm**.** In the UV region, Films with lower Al concentrations (2% and 8%) show slightly higher transmittance than those with 4%. The 4% film has the lowest UV transmittance (i.e., highest UV absorbance). However, in the visible region, Aluminum concentration has minimal effect on transmittance. All samples converge to almost the same transparency level. This suggests that, Al doping primarily affects defect states and absorption transitions in the UV range. But does not significantly change the transparency of ZnSe in the visible region. The films are suitable for applications requiring good optical clarity (e.g., windows, lenses, and optoelectronics).

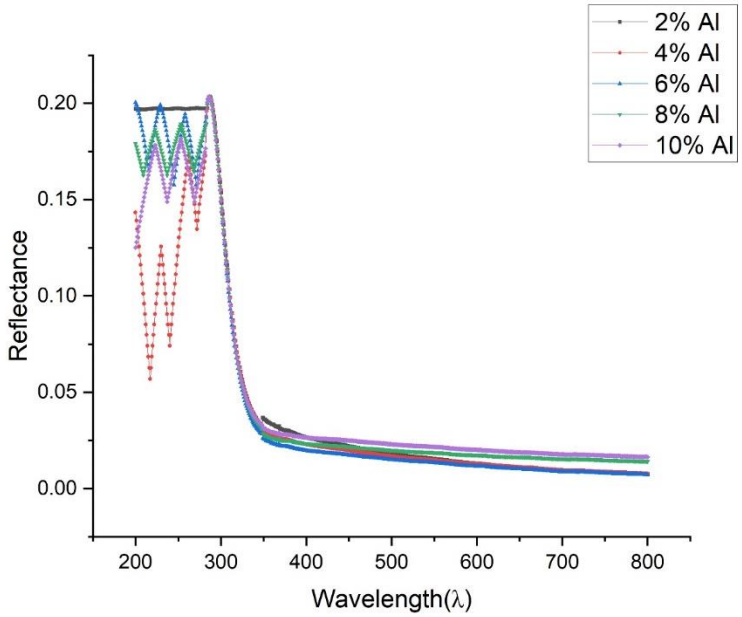

Fig 4.4: A graph of Reflectance against wavelength

The graph displayed a reflectance spectra of aluminum-doped ZnSe thin films with 2%, 4%, 6%, 8%, and 10% Al across the wavelength range 200–800 nm. The oscillations ("zig-zag patterns") correspond to interference effects, common in thin films due to multiple internal reflections and film thickness variation [Abdul, 2007]. The magnitude of reflectance varies slightly with aluminum concentration: 2% and 10% Al show the highest UV reflectance while 4% Al shows the lowest reflectance in this region. This is an indication that; Al concentration slightly affects surface roughness or refractive index in the UV range.

At very Low Reflectance in the Visible Region (400–800 nm) reflectance stabilizes at 0.00–0.03, which is extremely low. This means that the films are highly transparent and weakly reflective in the visible region. This behaviour aligns with the transmittance graph (figure 4.3, which shows high visible transparency).

Within the UV region, reflectance varies noticeably with Al concentration (stronger optical interference and higher reflectivity for 2% and 10% Al) while in the visible region, all samples show similar, very low reflectance, meaning doping does not significantly affect optical behaviour there. Thus, aluminum doping mainly affects UV optical response rather than visible-light reflectance.

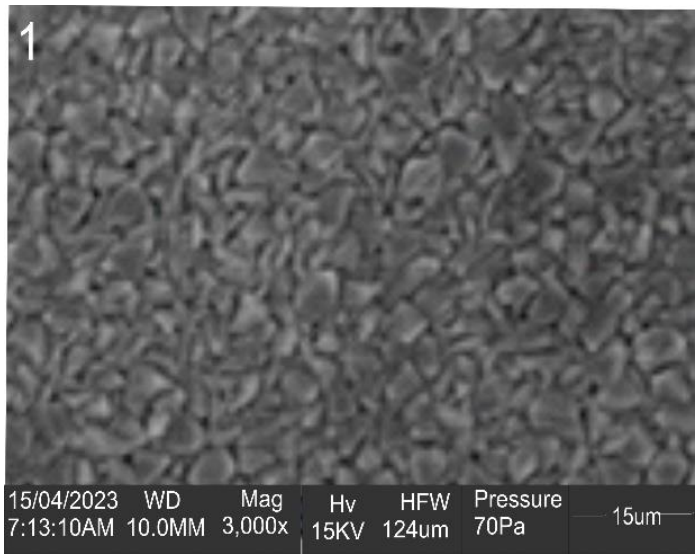

Fig 4.5: SEM Image of Sample containing 2% of Al

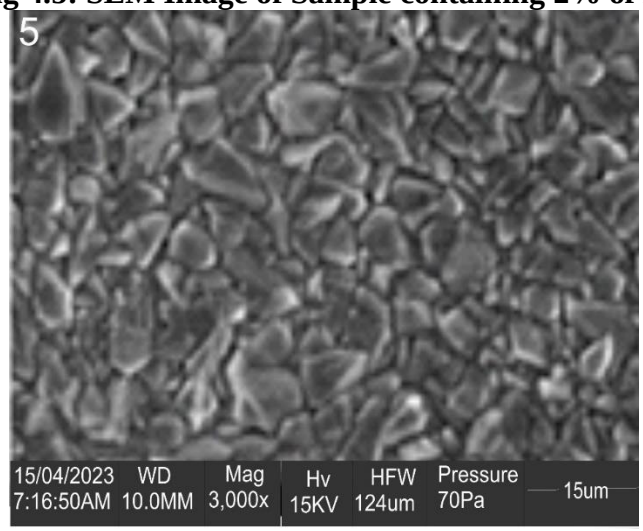

Fig 4.6: SEM Image of Sample containing 10% of Al.

Scanning Electron Microscopy (SEM) was employed to examine the surface morphology of the aluminum-doped zinc selenide (ZnSe:Al) thin films. Elemental and compositional analyses were carried out using a JOEL-JSM 7600F microscope. SEM imaging was performed at a magnification of 3000x, under a pressure of 70 Pa, and with an accelerating voltage of 15 kV. The SEM image reveals a densely packed and uniformly distributed granular surface morphology. The film appears to be continuous and well-covered, with no visible cracks, pinholes, or major voids, indicating good film formation and adhesion to the substrate.

The micrographs of the ZnSe:Al films (Figures 4.5 and 4.6) reveal pronounced grain formation, with noticeable differences in grain size between the samples. The micrograph also displays closely packed grains with irregular but predominantly rounded shapes. The grains are interconnected, forming a compact microstructure. This suggests a polycrystalline nature of the thin film. The film containing 2% Al exhibited a slight reduction in grain size compared to the other sample, which may be attributed to the variation in aluminum concentration (Kayed et al., 2019).

Structural implications of the displayed SEM result reveals the compact morphology with minimal porosity indicates good densification, which is favorable for: enhanced electrical conductivity, improved optical uniformity and reduced scattering losses. While the presence of larger grains (figure 4.6) suggests: reduced grain boundary scattering, potential improvement in charge carrier mobility and enhanced crystallinity.

Conclusion

Aluminum-doped zinc selenide (ZnSe:Al) thin films were successfully synthesized using the chemical bath deposition (CBD) technique, with zinc acetate dihydrate employed as the zinc ion precursor and concentrated hydrochloric acid serving as the complexing agent. Structural analysis revealed that increasing the aluminum doping concentration led to a reduction in both the number and intensity of diffraction peaks, indicating that higher Al content tends to suppress the crystallinity of the ZnSe thin films and results in a more disordered structure.

Optical studies showed that all the synthesized thin films exhibited high absorbance in the ultraviolet (UV) region, suggesting their potential suitability for UV-blocking and optoelectronic applications. In contrast, the films displayed low absorbance in the visible region, indicating good transparency. Furthermore, while the aluminum concentration influenced the position and intensity of the UV absorbance peaks, it had minimal effect on absorption within the visible-light region.

References

Abdul, A. (2007). "*Physical Optics: Principles and Practice".* CRC Press, London: 30-31.

Atikur, Md. Rahman. (2014), "*A review on Semiconductors Including Applications and Temperature Effects in Semiconductors*". American Scientific Research Journal for Engineering, Technology, and Sciences, 7(1), DOI: 10.1080/ 14484846.2016. 1264347

Gemechis Megersa Jigi, Tizazu Abza, Asnake Girma, (2021) "*Synthesis and Characterization of aluminum dope zinc sulfide (Al:ZnS) thin films by chemical bath deposition techniques*" Journal of Applied Biotechnology and Bioengineering. Volume 8 Issue 2

Gueymard C. A. (2004). *The sun's total and spectral irradiance for solar energy applications and solar radiation models.* Solar Energy, 76: 423-453.

Hawar Abdulrahman Rashid, Najmaldin Ezaldin Hassan. (2024)"*Toxic Gases and Human Health: A Comprehensive Review of Sources, Health Effects, and Prevention Strategies*" Journal of Materials Science Research and Reviews. DOI: 10.9734/ jmsrr/ 2024/ v7i4354, Page: 612-622, Issue: 2024 - Volume 7 [Issue 4]

Jérôme, F. (2025). "*Recreating Edmond Becquerel electrochemical actinometer*". Archives Des Sciences Journal 58(2)

Kassim A, Soon Min H., Wee Tee T., Shariff A., Saravanan K. & Saravanan N. (2011). *Chemical bath Deposition of ZnSe Thin Films: SEM and XRD Characterization. European Journal of Applied Sciences, Vol. 3(3): 113-116.*

Kayed T.S., Qasrawi A.F., & Elsayed A.K. (2019). "*Structural, Optical, Dielectric and Electrical Properties of Al-Doped ZnSe Thin Films".* Journal of Electronic Materials. doi.org/10.1007/s11664-019-07055-3.

Nasir EM. *Surface morphology and structural properties of ZnS and ZnS:Al thin films*. International Journal of Innovative Research in Science, Engineering and Technology; 3(1).

Nelson J. (2003). *The Physics of solar cells,* London, Imperial College Press, 23-25.

Okoli D.N. 2012 "*Growth and Characterization of PbSe Thin Films Prepared By Chemical Bath Deposition Technique*" Research Journal of Chemical Sciences. ISSN 2231-606X

Isi P.O., Ekpunobi A.J, Okoli D.N. (2021) "*Optical and electrical properties of fabricated dye sensitized solar cells based on extract from kolanut (Cola Acuminta)*". International Journal of Advances in Engineering and Management (IJAEM). Volume 3, issue7 page 3803-3822. Wwwijaem.net. ISSN 2395-5252

Pankove JI. (1991) "*Wide band gap semiconductors materials,* solid thin films. 1991.

Isi, P.O., Okwuoa, C.O., Jeroh, D.M. (2023) "*Growth and Characterization of Aluminum Doped Zinc Selenide (ZnSe:Al) Thin Films*" Volume 6, Issue 1, ISSN: 2664-0821

Rastkar, A, R., Nikham, A.R. and Shokri, B. (2009). *"Characterization of copper Oxide nanolayers deposited by direct current magnetron sputtering". Thin Solid Films, 517: 5464-5467.*

Sagadevan S. and Isha Das (2016). "*Chemical bath deposition (CBD) of zinc selenide (ZnSe) thin films and characterization*", Australian Journal of Mechanical Engineering 15(3):1-6Vol. 2(8), page 72-75,

Xia, M.; Liu, C.; Zhao, Z. (2015), "*Formation and optical properties of ZnSe and ZnSnanocrystals in glasses".* J. Non-Cryst. Solid, 429, 79-82, DOI:https://10.1016/j.jnoncrysol.2015.08.034.

Zhang, Q.; Li, H.; Ma, Y.; Zhai, T. (2016), "*ZnSe nanostructures: Synthesis, propertiesan applications*". Progress in Materials Science, 83, 472-535, DOI:https://10.1016/j.pmatsci.2016.07.005.